UNIVERSIDAD DE LAS PALMAS
DE GRAN CANARIA

A SIMPLE MODEL TO ESTIMATE ACTIVE FLUX IN RELATION TO ZOOPLANKTON LUNAR CYCLES IN SUBTROPICAL WATERS

Trabajo de Investigación presentado por:
Gara Franchy Gil

Dirigido por:
Santiago Hernández León

18 de Diciembre de 2009

PROGRAMA DE MÁSTER EN OCEANOGRAFÍA
BIENIO 2007-2009

PROGRAMA DE DOCTORADO EN OCEANOGRAFÍA
BIENIO 2008-2010

A simple model to estimate active flux in relation to zooplankton lunar cycles in subtropical waters

Gara Franchy[1,*] and Santiago Hernández-León[1]

[1]Biological Oceanography Laboratory, Facultad de Ciencias del Mar, Universidad de Las Palmas de Gran Canaria.

*E-mail: gfranchy@becarios.ulpgc.es

Abstract

Epipelagic mesozooplankton biomass was studied during the late winter bloom in the Canary Islands waters. As observed in previous works in the area, biomass peaked around every full moon within the productive season. This occurs because during the lunar illuminated phase, to avoid predation, diel vertical migrants do not reach the shallower layers (0-100 m) of the ocean, while during the dark period migrants reach these shallower waters. As a consequence, the epipelagic mesozooplankton grows without predation pressure around full moon, and decrease for the period of the dark phase of the lunar cycle because of consumption by migrants. In order to model this cycle of predation, a simple equation was used to simulate mesozooplankton biomass during the bloom. The outcomes of this model showed significant correlations between the true and predicted biomass at different growth and mortality rates during the 2006 year bloom. The estimated active flux values for this period were comparable with gravitational flux values in the same area. These results indicate that active flux represents an important and unaccounted flux of carbon to the mesopelagic zone.

Introduction

The Canary Islands are located in subtropical waters, in the Canary Current influence zone, which is a cold current flowing towards the equator as a branch of the North Atlantic Subtropical Gyre. These waters are oligotrophic because of the presence of a strong thermocline that prevents the nutrient diffusion to the euphotic layer. However, the erosion of the thermocline occurs after the winter because of the surface cooling, promoting the so-called “late winter bloom” (Menzel and Ryther, 1961; De León and Braun, 1973).

The phytoplankton bloom during winter is observed as an increase in chlorophyll (De León and Braun, 1973; Braun, 1980; Arístegui, 1990; Arístegui *et al*., 2001), followed by mesozooplankton (Arístegui, 1990; Arístegui *et al*., 2001; Hernández-León *et al*., 2004).

In his turn, the epipelagic mesozooplankton supports a large predation pressure by the diel vertical migrant organisms, which reach the shallower layers at night. During the day, they remain in deep waters at 400-500 meters to avoid predation (Moore, 1950; Uda, 1956; Stich and Lampert, 1981). The migrants response to the light intensity (Kampa and Boden, 1954) explains the relationship between the zooplankton and the lunar cycle recently observed in Canary Islands waters (Hernández-León, 1998; Hernández-León *et al*., 2001; Hernández-León *et al*., 2002; Hernández-León *et al.*, 2004). When the maximum illumination takes place, during the full moon, these organisms do not reach the shallower waters to avoid predation by nektonic organisms, and the epipelagic mesozooplankton grows without predation pressure. However, during new moon the vertical migrants occupy at the first hundred meters of the water column and feed on the epipelagic mesozooplankton, whose biomass drops.

The consumption of epipelagic zooplankton and the transport of this organic matter to the mesopelagic zone constitute the active flux of the biological pump, which is a rather complex mechanism that involves the gut flux (Angel, 1989) (the transport due to the release of faeces below the mixed layer), carbon dioxide respiration (Longhurst *et al.*, 1990), dissolved organic carbon excretion (Steinberg *et al.*, 2000) and mortality (Zhang and Dam, 1997) at the mesopelagic realm.

The few values available at present mainly based on respiration at depth indicate that the active downward carbon flux is highly variable and ranges in the 4-70% of the gravitational flux (Hernández-León and Ikeda, 2005a). However, DVMs account for the

control of 5-10% of the daily epipelagic zooplankton production (Hopkins *et al.*, 1996) and this ingested food is efficiently transported downward (Pearre, 2003).

However, most of the research about the downward flux of carbon in the ocean was centered on the so-called gravitational flux, the transport due to the sedimentation of the particulate organic carbon production from the euphotic layer to the mesopelagic zone, and the role of these rather large organisms (mesozooplankton and micronekton) in the ocean carbon sequestration has been almost neglected.

The different predatory scenarios during the winter bloom in the Canary Current provide an opportunity to study the response of plankton communities to the winter enrichment, as well as the predatory cycle related to the lunar phase. Active flux can be measured by analyzing the defecation, respiration, excretion and mortality of DVMs in the mesopelagic zone. Another approach is the knowledge of feeding by DVMs in the shallower layers, assuming that a large percentage of this energy is transported to the mesopelagic zone. However, these measurements are a rather difficult task which is outside the scope of the present work. Therefore, as a first step to assess the importance of DVMs in the transport of carbon to deep waters, we simulated the observed zooplankton lunar cycle and we estimated the consumption of carbon by the migrant biota. We calculated mortality due to DVMs assuming this value proportional to the lunar illumination. The results show that values of active flux could be in the order of values for gravitational flux.

Material and methods

Hydrological parameters, chlorophyll and zooplankton biomass were measured weekly at five stations around Gran Canaria Island (Canary Islands). Sampling was performed from October 2005 to June 2006 at the edge of the island shelf (Fig. 1).

Vertical profiles of temperature, conductivity and fluorescence were obtained using a CTD probe (SBE25 Sea-Bird Electronics) equipped with an *in situ* fluorometer. Phytoplankton chlorophyll was derived from depth profiles of *in situ* fluorescence, calibrated with samples collected at 15 m depth with a Niskin bottle. Chlorophyll was determined filtering 500 mL of seawater through Whatman GF/F filters which were preserved in liquid nitrogen until analysis in the laboratory. Pigments were extracted in cold acetone (90%) for 24 h. These extracts were acidified allowing chlorophyll and

phaeopigments to be independently measured in a Turner Design fluorometer previously calibrated with pure chlorophyll (Yentsch and Menzel, 1963).

Zooplankton was captured in oblique hauls with a Bongo net equipped with 200 µm mesh nets. The sampler was hauled during daylight hours from 90 m depth to the surface at a speed of about 2-3 knots. A General Oceanics flowmeter was used to measure the volume of water filtered by the net. One of the zooplankton samples was preserved in 4% buffered formaline and used for taxonomical collection. The second sample was transported in cold to the laboratory and dry weight measured using a standard procedure (Lovegrove, 1966).

In order to estimate predation by DVMs, we performed a simple and conservative model to simulate epipelagic mesozooplankton biomass during the winter bloom using the criteria of previous works (Hernández-León *et al.*, 2002, 2004), considering

$$P=(B_1-B_0)+M \quad (1)$$

where P is production of zooplankton, B_1 and B_0 are their biomass at time 1 and 0 respectively, and M is mortality. Then,

$$B_1=B_0 + (B_0 \times g) - (B_0 \times m) \quad (2)$$

being g the growth rate and m the mortality rate.

The initial biomass value, B_0, was considered as a real pre-bloom biomass value, just before the mesozooplankton biomass started to increase, and mortality rate, m, was set as function of the moon illumination. For the period of new moon, DVMs predation produces the maximum epipelagic mesozooplankton mortality rate. Contrary, within full moon period maximum illumination occurs, so that predation diminishes and the epipelagic mesozooplankton mortality rate is minimal.

As a first approach, daily growth rate was set constant with a conservative value of 0.1 d^{-1}, while mortality rate was set as a function of the lunar illumination, using increasing maximum values to test the better correlations between the true and predicted biomass.

A second simulation was performed by setting the growth rate as a function of the lunar illumination too. Different maximum values were also tested at different phases of the moon in order to find the better correlation coefficients. A third simulation was made ascribing different maximum growth rates to each observed peak during the bloom.

Maximum growth rates were set according to Hirst and Lampitt (1998) ranging from 0.1 d^{-1} to 0.3 d^{-1}. The latter value is the growth rate predicted by Huntley and Lopez (1992) for a water temperature of 18ºC, the average temperature in the euphotic layer during the bloom. Minimum values of growth and mortality rates, 0.01 to 0.04 d^{-1}, were taken from the literature (Hirst and Lampitt, 1998; Hirst and Kiørboe, 2002).

Finally, the daily community mortality was estimated multiplying the biomass by the mortality rate each day, and the mean community mortality for each bloom peak was assumed to be the average active carbon flux value during that peak. Once the best simulation was obtained with the 2006 year data, the model was applied to the 2005 year data, and mean community mortality was also assessed.

Results

Mixing in the water column started in December-January and the higher values of chlorophyll were observed at the end of January (Fig. 2a), coinciding with temperature below 19^{o}C, which indicate the suitable mixing conditions for the bloom (see also Hernández-León *et al.*, 2004; Moyano *et al.*, 2009). Mesozooplankton biomass, however, showed an increasing trend from December through March, displaying a clear lunar cycle pattern (Fig. 2b).

Zooplankton should continuously increase during the development of the phytoplankton bloom. However, a periodic increase and decrease in epipelagic mesozooplankton biomass coupled with every lunar cycle was observed. Standardizing the biomass values during the winter bloom (from January to March), taking maximum values of biomass in every lunar cycle as 100%, we observed that biomass was significantly lower during the first quarter of the moon (from new moon to crescent moon) and maxima during the illuminated phases of the lunar cycle (Fig. 3). A significant positive correlation (r^2=0.533, $p<0.05$) was also found between lunar illumination and mesozooplankton biomass.

The results of the model to estimate DVMs-induced mesozooplankton mortality showed a lag of 11 days between true and predicted biomass when growth rate was set constant and mortality as a function of lunar illumination (Fig. 4). This lag only disappeared when the growth rate was also set as a function of the lunar illumination, and its maximum value located ten days before full moon, during the waxing moon (Fig. 5). Using different maximum growth rates for every peak, we obtained a more

realistic match between true and predicted biomass (Fig. 6). In any case, good agreement was observed between the predicted and the measured mesozooplankton biomass in the last two cases (Table 1). The use of the same maximum growth and mortality rates for the three mesozooplankton biomass peaks (Table 1, upper pannel), or different maximum growth and mortality rates for every peak (Table 1, lower pannel) did not promote quite different values of community mortality. Those values ranged between 1.6 and 2.8 mmolC m^{-2} d^{-1} for the first peak, at the beginning of the bloom, and 2.7-6.3 mmolC m^{-2} d^{-1} during the rest of the bloom.

Validation of the results of this simple model during the 2005 winter and spring (Fig. 7) showed a similar distribution of the true and predicted mesozooplankton biomass for the last two peaks. However, the model could not simulate the first peak as it was induced by a Saharan dust deposition event (see discussion). Correlation values were low, and no significance was encountered because of the scarceness of data. Nevertheless, average community mortality values were comparable with the 2006 year values (Table 2).

Discussion

The results show a clear lunar cycle in mesozooplankton during the late winter bloom in these subtropical waters. The different peaks of mesozooplankton biomass were linked to the lunar cycle as observed in previous works in the area (Hernández-León *et al.*, 2002, 2004), although these increases were not always observed during the same months. The processes engaged in the development of the bloom in subtropical waters are rather complex and still not fully understood.

In contrast to some previous works, the zooplankton lunar pattern observed during late winter in the present work showed biomass peaks which were centred near the full moon (Fig. 2b and 3). Hernández-León *et al.* (2004) found the biomass increase during the illuminated phase of the lunar cycle and the maximum near the waning moon. They explained this pattern as the effect of high growth rates of zooplankton counteracting mortality until the latter surpassed the former as darkness progressed through the lunar cycle. Thus, the interplay between both rates promotes the biomass to peak around the full moon.

Mesozooplankton biomass simulation with the simple model developed in this work showed high correlation values between the true and predicted biomass in the 2006

sampling (Table 1). However, during 2005 a Saharan dust deposition event occurred, and only two peaks could be included in the simulation, promoting lower correlation values (Table 2) than during the 2006 event. Our simple model did not simulate the first peak of the bloom produced by the fertilization of the Saharan dust because this phenomenon was not considered in the growth and mortality equations.

Using this model, we were able to assess mortality during the different mesozooplankton lunar cycles. Growth rates values used to simulate the bloom (Table 1) were approximately half the value of 0.3 d^{-1} predicted by Huntley and Lopez (1992) for the average temperature in the euphotic layer during the bloom. Therefore, we consider our approach as conservative. The values of the first peak observed at the beginning of the bloom in 2006 (range 1.6-2.8 mmolC m^{-2} d^{-1} in January, Table 1) was comparable with two previous estimations (Hernández-León *et al.*, 2002, 2004) obtained north of the Canary Islands, which gave average values of 1.9 and 2.9 mmolC m^{-2} d^{-1} for May, 1999 and February-March, 2000, respectively. The second and third peaks found in 2006 and the first and second peaks found in 2005 showed considerably larger average values (range 2.7-6.3 mmolC m^{-2} d^{-1}). In the oceanic zone of the Canary Current, north of the Canaries, average values for gravitational flux (Neuer *et al.*, 2007) using sediment traps were 0.7 mmolC m^{-2} d^{-1}, whereas in Bermuda was 2.4 mmolC m^{-2} d^{-1} (Michaels and Knap, 1996; Karl *et al.*, 2001), and 2.3-2.4 mmolC m^{-2} d^{-1} in Hawaii (Karl *et al.*, 1996; Benitez-Nelson *et al.*, 2001). Thus, our estimates of mortality during the first peak in 2006 (similar to previous ones) are similar to average values of gravitational flux in Hawaii and Bermuda in a non-bloom scenario. However, these values of mortality are 2-4 fold greater than the average values of gravitational flux in the Canary Current given by Neuer *et al.* (2007) and in the order or higher than export flux (0.7-2 mmolC m^{-2} d^{-1}) found by Alonso-González *et al.* (2009) also in the Canary Current from spring to autumn. Moreover, our average values during the bloom were 2-4 fold greater than the highest value of gravitational flux (~1.3 mmolC m^{-2} d^{-1}) recorded in the Canary Current by Neuer *et al.* (2007), and in the order or higher than the highest records of gravitational flux observed in the Canary basin (3-4 mmolC m^{-2} d^{-1}) by Alonso-González *et al.* (2009), and in Bermuda (Michaels and Knap, 1996) and Hawaii (Karl *et al.*, 1996) of about 6 mmolC m^{-2} d^{-1}.

Different observations, recently reviewed by Pearre (2003), indicate that diel migrants reach the shallower layers at dusk, feed until their guts are full and then, asynchronously, migrate downward to avoid predation. Moreover, gut clearance rates in micronekton was observed to be long enough for the downward migration to have been completed before evacuation occurs (Merret and Roe, 1974; Baird *et al.*, 1975;

Gorelova and Kobylyansky, 1985; Angel and Pugh, 2000). In addition, faecal matter of mesopelagic fish show fast sinking rates (average of 1028 m d^{-1}), much higher than copepod or euphausiid faecal pellets (Robison and Bailey, 1981). The latter authors also observed that the release of dissolved organic compounds is low and does not represent a significant output during sinking. This rapid sinking and slow dissolution promote a higher efficiency in the flux of carbon to the deep-sea. Moreover, this community is composed in a large percentage of fishes and these organisms produce precipitated carbonates which are defecated and transported downward (Wilson *et al.* 2009). Thus, if we assume that a high percentage of preyed upon mesozooplankton at shallower layers is transported to the mesopelagic zone by DVMs, the estimated active flux values are, at least, of the same magnitude than the gravitational flux normally found in subtropical waters.

The role of this rather large fauna was scarcely considered in previous works about active flux. Diel migrants were normally sampled using unsuitable nets for micronektonic organisms. This bias in the measurement of DVM biomass could give rise to an important underestimation of the active flux in the ocean. In this sense, Hidaka *et al.* (2001) assessed active flux by mesozooplankton and micronekton in the western equatorial Pacific Ocean. Their results showed that flux due to micronektonic organisms was 56-60% of total active flux. Therefore, values of this flux based only on the mesozooplankton fraction (see Hernández-León and Ikeda, 2005a) are clear underestimate. Unfortunately, sampling micronekton is rather difficult and time-consuming but, as indirectly observed in the present work, their transport is of paramount importance for the assessment of the role of the biological pump in the ocean.

In summary, we show that downward carbon transport in subtropical waters does not end with the sinking of the organic carbon produced in the shallower layers. In fact, the process is much more complex and part of the production is shunted to the mesopelagic zone by DVMs. Our results shed some light on the uncoupling between primary production and particle export flux in the ocean (Michaels *et al.*, 1994a; Karl *et al.*, 1996) and may explain the 30 days periodicity in the gravitational flux observed in the oceanic waters of the Canary Current (Khripounoff *et al.*, 1998). In addition, this active flux could explain, at least in part, the unaccounted downward organic flux promoting the carbon demands of bacteria and zooplankton in the mesopelagic zone (Steinberg *et al.*, 2008). Moreover, geochemical estimates of new production are in the range of 6.8-14.6 mmolC m^{-2} d^{-1} (Jenkins, 1988; Michaels *et al.*, 1994b; Jenkins and Doney, 2003), much higher than sediment trap measurements but near the addition of

gravitational and our conservative estimates of active fluxes. Thus, our results suggest a pivotal role of epipelagic zooplankton and DVMs in the biological pump and gives insight into the fate of a bloom. In any case, the lunar cycle-linked active flux described here for subtropical oligotrophic waters represents an important and unaccounted flux of carbon to the mesopelagic zone which deserves further research. The finding of DVMs movements at 800-1300 m depth following the lunar cycle (van Haren, 2007), also gives insight into a ladder of migration (*sensu* Vinogradov, 1970) of valuable consequences for carbon transport to the deep sea.

Acknowledgements

This work was supported by the Project LuCIFer (CMT2008-03538/MAR) and the University of Las Palmas de Gran Canaria (ULPGC).

References

Alonso-González. I., Arístegui, J., Vilas, J.C. and Hernández-Guerra, A. (2009). Lateral transport of POC and consumption in surface and deep waters of the Canary Current: A box model study. Global Biogeochem. Cycles 23, GB2007 doi: 10.1029/ 2008GB003185.

Angel, M.V. (1989). Does mesopelagic biology affect the vertical flux? In: Berger, W.H., Smetacek, V.S. & Wefer, G. (eds), *Productivity of the Ocean: Present and Past*, Wiley, N.Y., pp. 155-173.

Angel, M.V. and Pugh, P.R. (2000). Quantification of diel vertical migration by micronektonic taxa in the northeast Atlantic. Hydrobiologia 440, 161-179.

Arístegui, J. (1990). La distribución de la clorofila *a* en aguas de Canarias. Bol. Inst. Esp. Oceanogr. 6 (2), 61-72.

Arístegui, J., Hernández-León, S., Montero, M.F. and Gómez, M. (2001). The seasonal planktonic cycle in coastal waters of the Canary Islands. Sci.Mar., 65 (Suppl. 1), 51-58.

Baird, R.C., Hopkins, T.L. and Wilson, D.F. (1975). Diet and feeding chronology of *Diaphus taaningi* (Myctophidae) in the Cariaco Trench. Copeia 1975, 356-365.

Benitez-Nelson, C., Buesseler, K.O., Karl, D.M. and Andrews, J. (2001). A time-series study of particulate matter export in the North Pacific Subtropical Gyre based on ^{234}Th: ^{238}U disequilibrium. Deep-Sea Research I, 48, 2595-2611.

Braun, J.G. (1980). Estudios de producción en aguas de las Islas Canarias. I. Hidrografía, nutrientes y producción primaria. Bol. Inst. Espa. Oceanogr., Tomo V: 147-154.

De León, A.R. and Braun, J.G. (1973). Ciclo anual de la producción primaria y su relación con los nutrientes en aguas canarias. Bol. Inst. Espa. Oceanogr., 167.

Gorelova, T.A. and Kobylyansky, S.G. (1985). Feeding of deep-sea fishes of the Family Bathylagidae. J. Ichthyol. 32, 264-274.

Hernández-León, S. (1998). Annual cycle of epiplanktonic copepods in Canary Island waters. *Fish. Oceanogr*. 7, 252-257.

Hernández-León, S., Almeida, C., Yebra, L., Arístegui, J., Fernández de Puelles, M.L. and García-Braun, J. (2001). Zooplankton abundance in subtropical waters: Is there a lunar cycle? *Sci. Mar.* 65, 59-64.

Hernández-León, S, Almeida, C., Yebra, L. and Arístegui, J. (2002). Lunar cycle of zooplankton biomass in subtropical waters: biogeochemical implications. *J. Plankton Res.* 24, 935-939.

Hernández-León, S., Almeida C., Bécognée, P., Yebra, L. & Arístegui, J. (2004). Zooplankton biomass and indices of grazing and metabolism during a Late Winter Bloom in subtropical waters. *Mar. Biol*. 145, 1191-1200.

Hernández-León, S. and Ikeda, T. (2005). Zooplankton Respiration. In: Williams, P.L.B. & del Giorgio, P. (eds), *Respiration in aquatic ecosystems*, Oxford University Press, pp. 57-82.

Hidaka, K., Kawaguchi, K., Murakami, M. and Takahashi, M. (2001). Downward transport of organic carbon by diel migratory micronekton in the western equatorial Pacific: its quantitative and qualitative importance. *Deep-Sea Res. I*., 48: 1923-1939.

Hirst, A.G. and Kiorboe, T. (2002). Mortality of marine planktonic copepods: global rates and patterns. Mar. Ecol. Prog. Ser. 230, 195-209.

Hirst, A.G. and Lampitt, R.S. (1998). Towards a global model of in situ weight-specific growth of marine planktonic copepods. Mar. Biol. 132, 247-257.

Hopkins, T.L., Sutton, T.T. and Lancraft, T.M. (1996). The trophic structure and predation impact of a low latitude midwater fish assemblage. *Prog. Oceanogr*. 38, 205-239.

Huntley M.E. and Lopez M.D.G. (1992). Temperature-dependent production of marine copepods: A global synthesis. Am Nat 140, 201-242.

Jenkins, W.J. (1988). Nitrate into the euphotic zone near Bermuda. Nature 331, 521-523.

Jenkins, W.J. and Doney, S.C. (2003). The subtropical nutrient spiral. Global Biogeochem. Cycles 17, 1110 doi: 10.1029/ 2003GB002085.

Kampa, E.M. and Boden, B.P. (1954). Submarine illumination and the twilight movements of a sonic scattering layer. Nature 174, 869-871.

Karl, D.M., Dore, J.E., Lukas, R., Michaels, A.F., Bates, N.R., and Knap, A. (2001). Building the long-term picture: the U.S. JGOFS time-series programs. *Oceanography* 14, 6-17.

Karl, D.M., Christian JR, Dore JE, Hebel DV, Letelier RM, Tupas LM and Winn C.D. (1996). Seasonal and interannual variability in primary production and particle flux at Station ALOHA. *Deep-Sea Res. II* 43, 539-568.

Khripounoff, A., Vangriesheim, A. and Crassous, P. (1998). Vertical and temporal variations of particle fluxes in the deep tropical Atlantic. *Deep-Sea Res I* 45, 193-216.

Longhurst, A.R., Bedo, A., Harrison, W.G., Head, E.J.H. and Sameoto, D.D. (1990). Vertical flux of respiratory carbon by oceanic diel migrant biota. *Deep-Sea Res*. 37, 685-694.

Lovegrove, T. (1966). The determination of the dry weight of plankton and the effect of various factors on the values obtained. In: Barnes H. (ed), *Some contemporary studies in marine science*, George Allen and Unwin, London, pp 429-467.

Menzel, D.W., and Ryther, J.H. (1961). Zooplankton in the Sargasso Sea off Bermuda and its relation to organic production. J. Du Conseil Pour L'Exploration De La Mer. 26: 250-258.

Merret, N.R. and Roe, H.S.J. (1974). Patterns and selectivity in the feeding of certain mesopelagic fishes. Mar. Biol. 28, 115-126.

Michaels, A.F., Bates, N.R., Buesseler, K.O., Carlson, C.A., and Knapp, A.H. (1994a). Carbon cycle imbalances in the Sargasso Sea. *Nature* 372, 537-540.

Michaels, A.F., Knap, A.H., Dow, R.L., Gundersen, K., Johnson, R.J., Sorensen, J., Close, A., Knauer, G.A., Lohrenz, S.E., Asper, V.A., Tuel, M. and Bidigare, R. (1994b). Seasonal patterns of ocean biogeochemistry at the U.S. JGOFS Bermuda Atlantic time-series study site. Deep-Sea Res I, 41, 1013-1038.

Michaels, A.F. and A.H. Knap (1996). Overview of the U.S. JGOFS Bermuda Atlantic Time-series Study and hydrostation S program. Deep-Sea Research II, 43, 157-198.

Moore, H.B. (1950). The relation between the scattering layer and the euphausiacea. Biol. Bull. 99, 181-212.

Moyano, M., Rodríguez, J.M. and Hernández-León, S. (2009). Larval fish abundance and distribution during the late winter bloom in the Canary Island waters. Fisheries Oceanography 18 (1), 51-61.

Neuer, S., Cianca, A., Helmke, P., Freudenthal, T., Davenport, R., Meggers, H., Knoll, M., Santana-Casiano, J.M., González-Dávila, M., Rueda, M.J. and Llinás, O. (2007).

Biogeogeochemistry and hydrography in the eastern subtropical North Atlantic gyre. Results from the European time-series station ESTOC. Prog. Oceanogr. 72, 1-29.

Pearre, S. (2003). The hunger/satiation hypothesis in vertical migration: history, evidence and consequences. Biol. Rev. 78, 1-79.

Robison, B.H. and T.G. Bailey (1981). Sinking rates and dissolution of midwater fish fecal matter. Mar. Biol. **65:** 135-142.

Steinberg, D., Carlson, C.A., Bates, N.R., Goldthwait, S.A., Madin, L.P., Michaels, A.F. (2000). Zooplankton vertical migration and the active transport of dissolved organic and inorganic carbon in the Sargasso Sea. *Deep-Sea Res. I* 47, 137-158.

Steinberg, D.K., B.A.S. Van Mooy, K.O. Buesseler, P.W. Boyd, T. Kobari, D.M. Karl (2008). Bacterial vs. zooplankton control of sinking particle flux in the ocean´s twilight zone. Limnol. Oceanogr. 53, 1327-1338.

Stich, H.B. and Lampert, W. (1981). Predator evasion as an explanation of diurnal vertical migration by zooplankton. Nature 293, 396-398.

Uda, M. (1956). Researches on the fisheries grounds in relation to the scattering layer of supersonic wave. J. Tokyo Unv. Fish. 42, 103-111.

van Haren, H. (2007). Monthly periodicity in acoustic reflections and vertical motions in the deep ocean. Geophys. Res. Letters 34, L12603 doi: 10.1029/2007GL029947.

Vinogradov, M.E. (1970). Vertical distribution of the oceanic Zooplankton. Israel Program for Scientific Translations, Jerusalem, 339 p.

Wilson, R.W., Millero, F.J., Taylor, J.R., Walsh, P.J., Christensen, V., Jennings, S., Grosell, M. (2009). Contribution of fish to the marine inorganic carbon cycle. Science 323, 359-362.

Yentsch, C.S. and Menzel, D.W. (1963). A method for the determination of phytoplankton chlorophyll and phaeophytin by fluorescence. Deep-Sea Res. 10, 221-231.

Zhang, X. and Dam, H. (1997). Downward export of carbon by diel migrant mesozooplankton in the central equatorial Pacific. *Deep-Sea Res. II,* 44, 2191-2202.

Figures Legend

Figure 1. Map of the study area showing the location of the 5 sampling stations around Gran Canaria Island, Canary Islands (Northeast Subtropical Atlantic).

Figure 2a. Time series of temperature (open circles) and chlorophyll (filled circles) in the mixed layer from October 2005 to June 2006. Vertical bars represent standard error.

Figure 2b. Time series of mesozooplankton biomass (filled circles) and lunar illumination (dashed line) from October 2005 to June 2006. Vertical bars represent standard error. Lunar illumination is scaled relative to maximum brightness. Observe the lunar cycle in mesozooplankton biomass as the mixing develops through winter (from December to March).

Figure 3. Standardized biomass (maximum value of biomass in each lunar cycle converted to 100%) during the late winter bloom in the Canary Island waters.

Figure 4. True (open circles) and predicted (filled circles) mesozooplankton biomass ($r=0.544$, $p>0.05$) according to the lunar illumination (dashed line) (upper figure). Growth rate was set constant (0.10 d^{-1}) and mortality rate was set as a function of the lunar illumination (lower figure).

Figure 5. True (open circles) and predicted (predicted circles) mesozooplankton biomass ($r=0.902$, $p<0.0001$) according to the lunar illumination (dashed line) (upper figure). Growth (full line) and mortality (dashed line) rates used to simulate the biomass in the upper figure are showed (lower panel). Maximum growth rate was set within waxing moon ($g=0.11$ d^{-1}) and maximum mortality rate was set within new moon ($m=0.08$ d^{-1}). Minimum mortality and growth rates were 0.01 d^{-1} within full moon and waning moon, respectively.

Figure 6. True (open circles) and predicted (filled circles) mesozooplankton biomass ($r=0.873$, $p<0.001$) according to the lunar illumination (dashed line) (upper figure). Maximum growth rate was set within waxing moon and it was different for every peak (first peak: $g_1=0.13$ d^{-1}; second peak: $g_2=0.15$ d^{-1}; third peak: $g_3=0.18$ d^{-1}) and maximum mortality rate was set within new moon and it was different for every peak too (first peak: $m_1=0.12$ d^{-1}; second peak: $m_2=0.15$ d^{-1}; third peak: $m_3=0.13$ d^{-1}). Minimum mortality and growth rates were 0.01 d^{-1} within full moon and waning moon, respectively.

Figure 7. True (open circles) and predicted (filled circles) mesozooplankton biomass (r=0.516, p=n.s.) according to the lunar illumination (dashed line) during the 2005 winter and spring (upper figure). Maximum growth rate was set within waxing moon and it was different for every peak (first peak: g_1=0.17 d^{-1}; second peak: g_2=0.21 d^{-1}) and maximum mortality rate was set within new moon and it was different for every peak too (first peak: m_1=0.18 d^{-1}; second peak: m_2=0.15 d^{-1}) (lower figure). Minimum mortality and growth rates were 0.01 d^{-1} within full moon and waning moon, respectively.

Figures and Tables

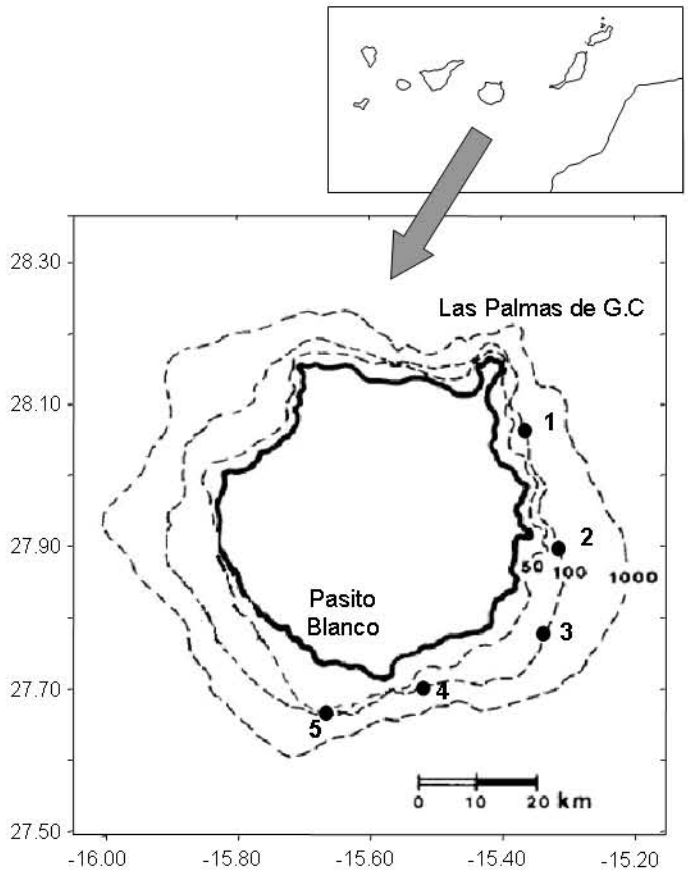

Figure 1

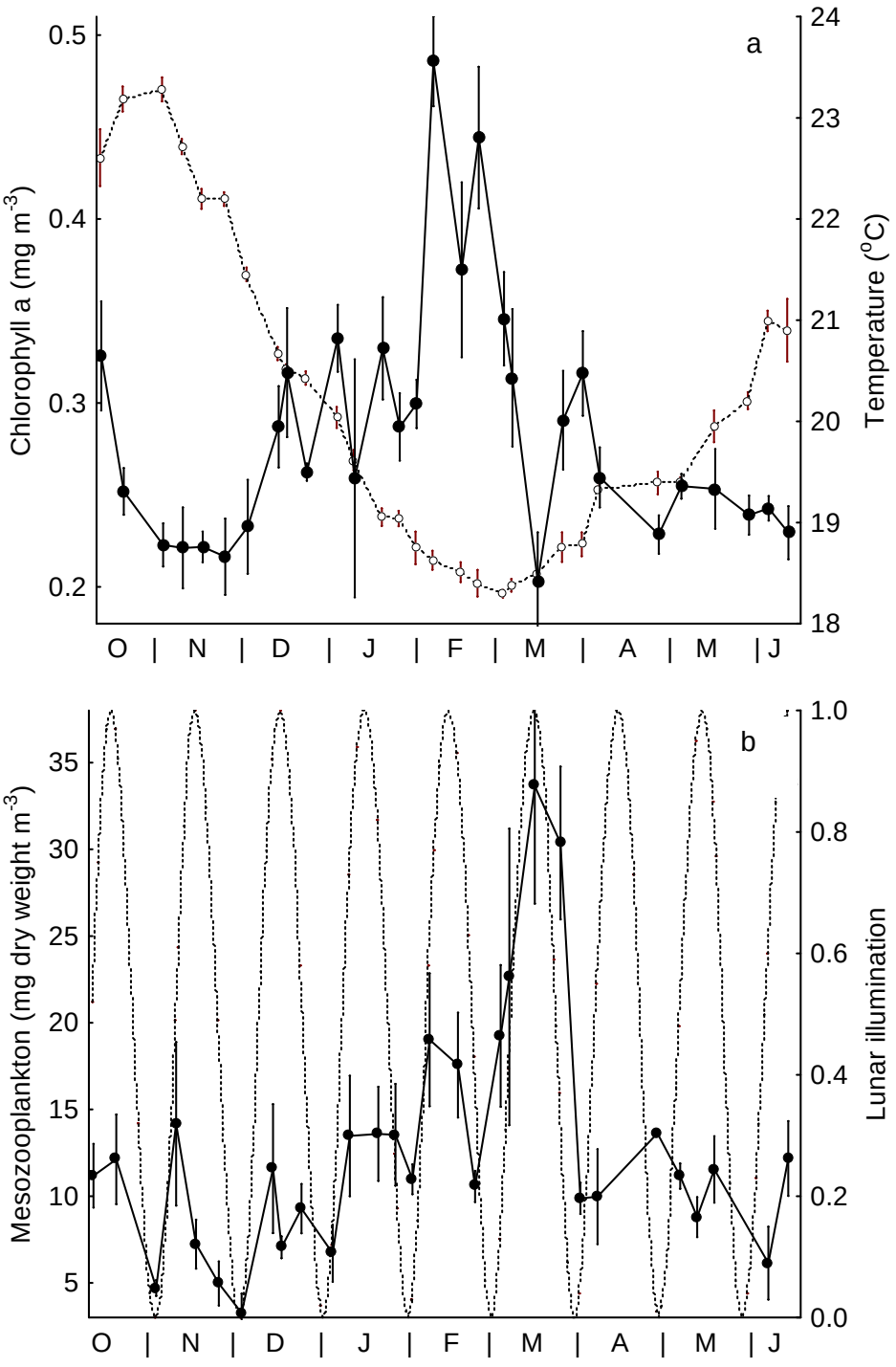
a
Chlorophyll a (mg m-3)
Temperature (°C)
0.5
0.4
0.3
0.2
24
23
22
21
20
19
18
O | N | D | J | F | M | A | M | J
b
Mesozooplankton (mg dry weight m-3)
Lunar illumination
35
30
25
20
15
10
5
1.0
0.8
0.6
0.4
0.2
0.0
O | N | D | J | F | M | A | M | J

Figure 2

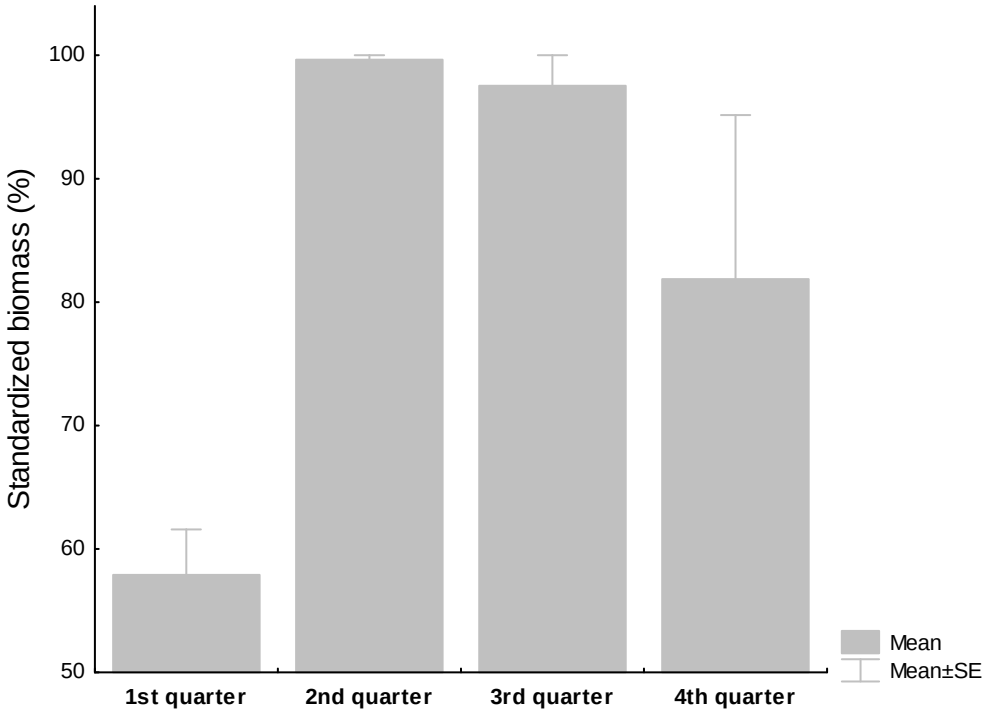
Standardized biomass (%)
100
90
80
70
60
50
1st quarter
2nd quarter
3rd quarter
4th quarter
Mean
Mean±SE

Figure 3

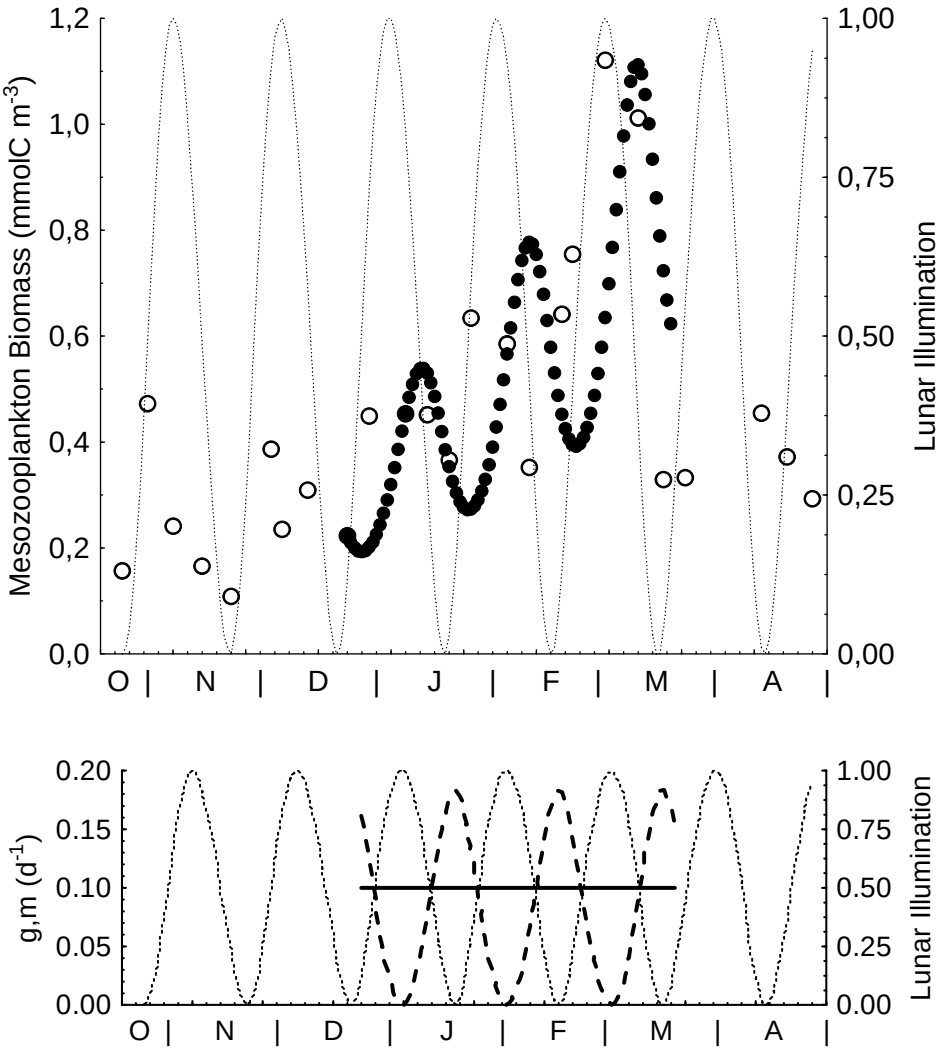
Mesozooplankton Biomass (mmolC m-3)
1,2
1,0
0,8
0,6
0,4
0,2
0,0
1,00
0,75
0,50
0,25
0,00
Lunar Illumination
O | N | D | J | F | M | A |
g,m (d-1)
0.20
0.15
0.10
0.05
0.00
1.00
0.75
0.50
0.25
0.00
Lunar Illumination
O | N | D | J | F | M | A |

Figure 4

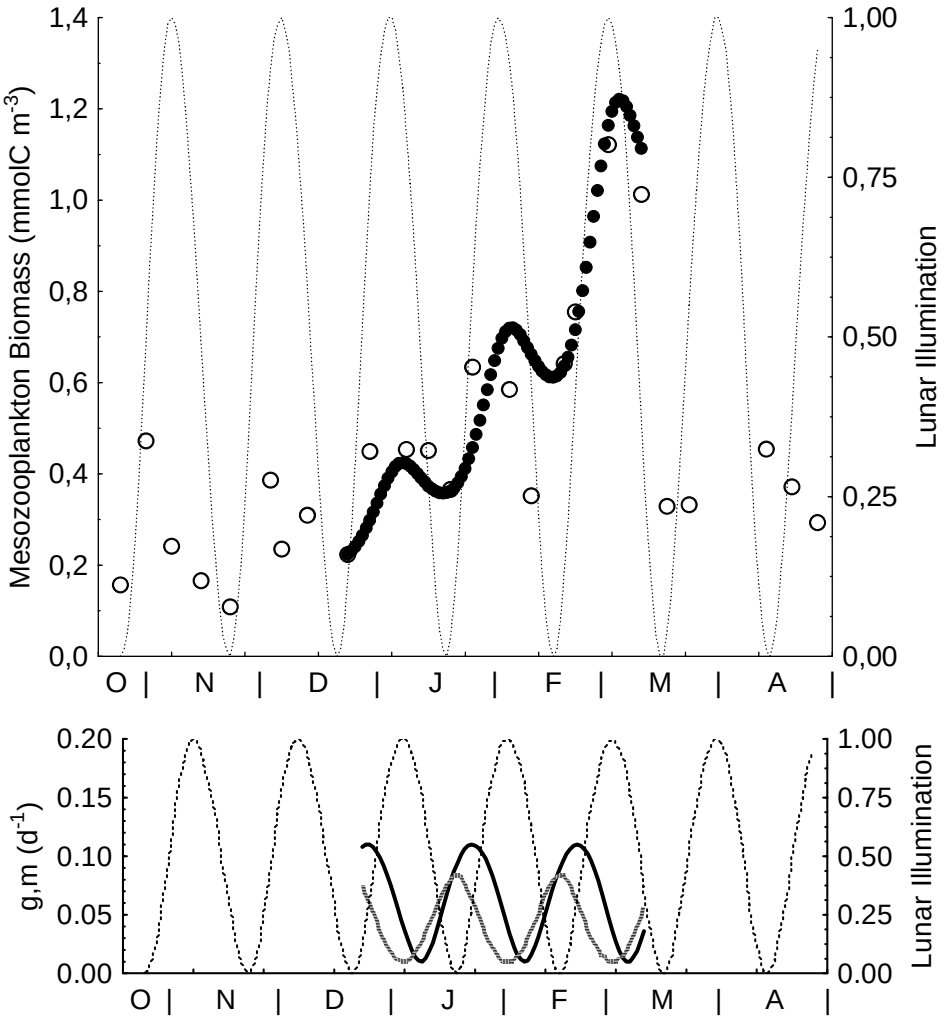
Mesozooplankton Biomass (mmolC m-3)
1,4
1,2
1,0
0,8
0,6
0,4
0,2
0,0
1,00
0,75
0,50
0,25
0,00
Lunar Illumination
O | N | D | J | F | M | A |
g,m (d-1)
0.20
0.15
0.10
0.05
0.00
1.00
0.75
0.50
0.25
0.00
Lunar Illumination
O | N | D | J | F | M | A |

Figure 5

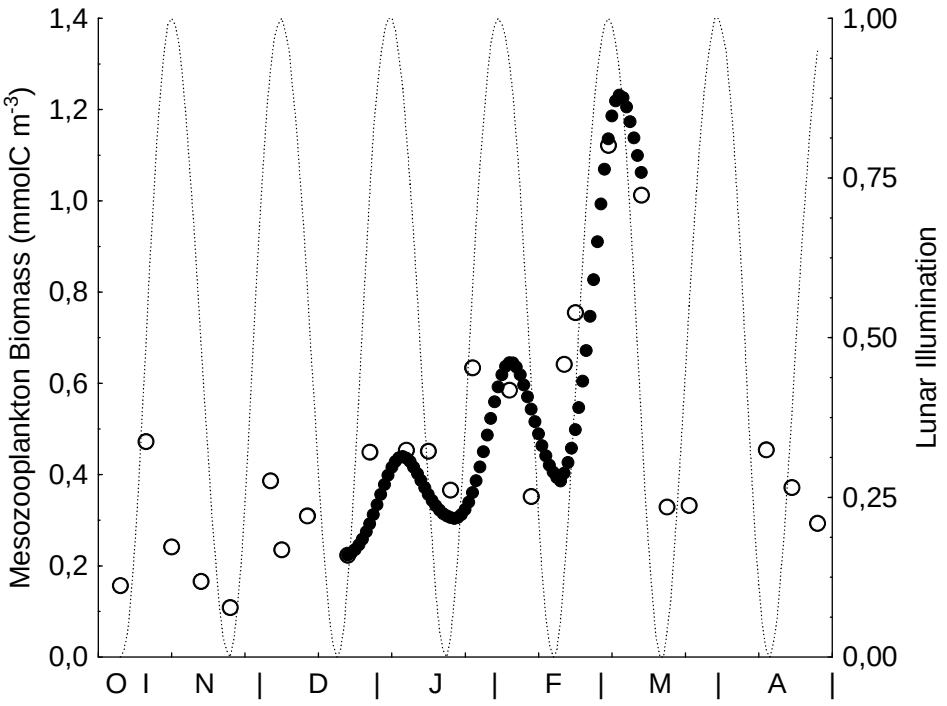
Mesozooplankton Biomass (mmolC m-3)
Lunar Illumination
1,4
1,2
1,0
0,8
0,6
0,4
0,2
0,0
1,00
0,75
0,50
0,25
0,00
O I N | D | J | F | M | A |

Figure 6

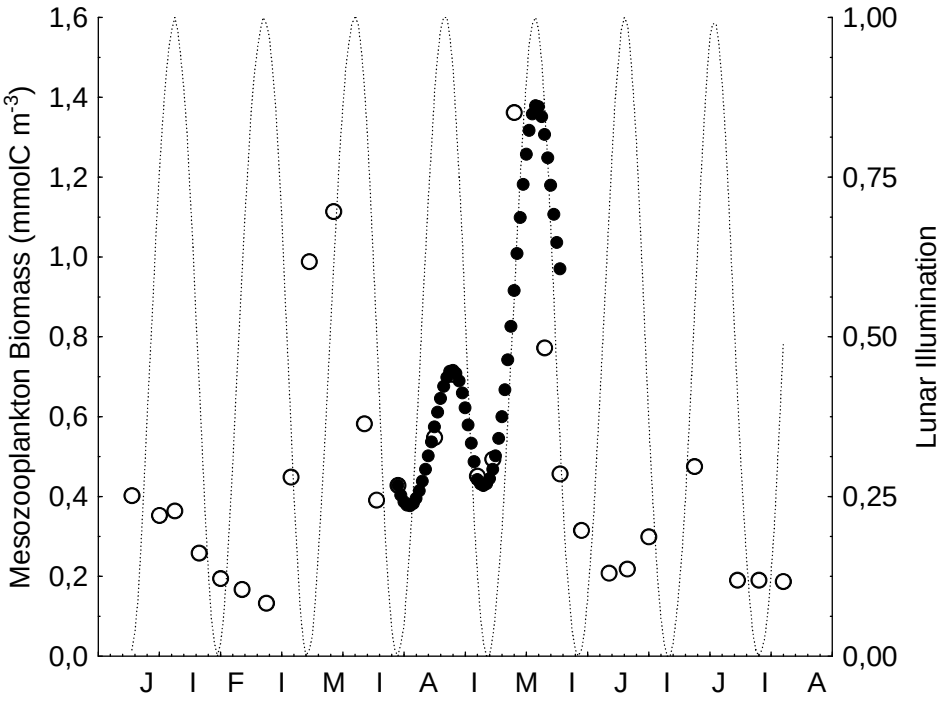
Mesozooplankton Biomass (mmolC m-3)
1,6
1,4
1,2
1,0
0,8
0,6
0,4
0,2
0,0
1,00
0,75
0,50
0,25
0,00
Lunar Illumination
J I F I M I A I M I J I J I A

Figure 7

Minimum Growth and Mortality Rate (d^{-1})	Maximum Growth Rate (d^{-1})			Maximum Mortality Rate (d^{-1})			Correlation	Significance	**Daily Community Mortality (mmolC m^{-2} d^{-1})**		
	g			m			r	p	M_1	M_2	M_3
0.01	0.11			0.08			0.902	<0.0001 (=0.00006)	**1.6**	**2.7**	**3.1**
0.02	0.13			0.09					**2.0**	**3.4**	**4.1**
0.03	0.14			0.10					**2.4**	**4.1**	**5.2**
0.04	0.15			0.11					**2.8**	**4.8**	**6.3**
	g_1	g_2	g_3	m_1	m_2	m_3	r	p	M_1	M_2	M_3
0.01	0.13	0.15	0.18	0.12	0.15	0.13	0.873	<0.001 (=0.0002)	**1.8**	**2.9**	**3.3**
0.02	0.14	0.16	0.19	0.13	0.16	0.14			**2.1**	**3.4**	**4.1**
0.03	0.15	0.17	0.20	0.14	0.17	0.15			**2.4**	**3.8**	**4.9**
0.04	0.16	0.18	0.21	0.15	0.18	0.16			**2.7**	**4.2**	**5.7**

Table 1. Daily Community Mortality values modeled in accordance with different growth and mortality rates in the case that the same maximum rate values were used during the bloom (upper panel) and in the case that different maximum rate values were used for every peak (lower panel) (g_1, m_1 and M_1 are first peak values; g_2, m_2 and M_2 are second peak values; and g_3, m_3 and M_3 are third peak values).

Minimum Growth and Mortality Rate (d^{-1})	Maximum Growth Rate (d^{-1})		Maximum Mortality Rate (d^{-1})		Correlation	Significance	**Daily Community Mortality (mmolC m^{-2} d^{-1})**	
	g_1	g_2	m_1	m_2	r	p	M_1	M_2
0.01	0.17	0.21	0.18	0.15	0.516	n.s.	**3.8**	**5.2**

Table 2. Daily Community Mortality values modeled during 2005 winter and spring. Different maximum rate values were used for every peak (g_1, m_1 and M_1 are first peak values; g_2, m_2 and M_2 are second peak values).